Thermochimica Acta 480 (2008) 15–21

Contents lists available at ScienceDirect

Thermochimica Acta

journal homepage: www.elsevier.com/locate/tca

The thermal stability of fully charged and discharged $LiCoO_2$ cathode and graphite anode in nitrogen and air atmospheres

Yan-Bing He [a,*], Zhi-Yuan Tang [a], Quan-Sheng Song [a], Hui Xie [a], Qiang Xu [a], Yuan-Gang Liu [b], Guo-Wei Ling [a]

[a] Department of Applied Chemistry, School of Chemical Engineering and Technology, Tianjin University, Tianjin 300072, China
[b] McNair Technology Co., Ltd., Dongguan City, Guangdong 523700, China

ARTICLE INFO

Article history:
Received 17 April 2008
Received in revised form
22 September 2008
Accepted 23 September 2008
Available online 1 October 2008

Keywords:
Lithium-ion batteries
Thermogravimetric (TG) and differential thermal analysis (DTA)
Thermal stability
$LiCoO_2$ cathode
Graphite anode

ABSTRACT

The thermogravimetric (TG) and differential thermal analysis (DTA) were used to investigate the thermal stability of fully charged and discharged $LiCoO_2$ cathode and graphite anode in nitrogen and air atmospheres. The results showed that the weight of charged and discharged $LiCoO_2$ cathode samples exhibited an obvious decrease between 100 and 120 °C in two atmospheres. The exothermic decomposition reaction of fully charged $LiCoO_2$ cathode occurred at 250 °C in two atmospheres. A small decomposition reaction of the discharged $LiCoO_2$ cathode occurred at 300 °C. When the temperature of samples was elevated to 600 °C, the weight of fully charged and discharged $LiCoO_2$ cathode in air atmosphere did not change; while the weight of samples in nitrogen atmosphere decreased. This was because the Co_3O_4 as the decomposition product of the cathodes could be reduced to CoO by the carbon black above 600 °C in N_2 atmosphere. The solid electrolyte interphase (SEI) film of fully charged and discharged graphite anode was decomposed at 100–120 °C in two atmospheres, and the weight loss of fully charged graphite anode at 100–120 °C was obviously less than that of the fully discharged graphite anode. When the samples were heated to 300 °C, there was no fierce exothermic reaction for the lithiated graphite anode in N_2 atmosphere, whereas an exothermic reaction in air atmosphere occurred rapidly.

1. Introduction

Lithium rechargeable batteries possess the advantages of long cycle life, high energy density and high voltage as compared with other secondary batteries [1,2]. Lithium-ion batteries are widely used in portable electronic devices and their electrochemical performance has been improved greatly. However, the safety of batteries is still the main concern of both consumers and manufacturers in the hybrid electric vehicle applications. The concern becomes more severe when the batteries work under abusive conditions such as high temperatures, high charge and discharge rates, and overcharge. More energy the batteries store, potentially more hazardous they will be. The main reason for firing and explosion of lithium-ion batteries can be attributed to rapid exothermic reactions of the electrode materials with the electrolyte components, which occur in batteries under abusive conditions, especially at high temperatures and overcharge. These reactions are known to be exothermic and can produce much heat and gas, which result in high pressure and temperature exceeding the enduring limits of the batteries [3–8].

It is well known that fully charged $LiCoO_2$ cathode materials with the electrolyte in lithium-ion batteries are unstable, and are easy to be decomposed to release oxygen at elevated temperatures. The evolved oxygen can then react with the organic solvent in the electrolyte (e.g. EC, DEC, EMC, DMC, etc.), which generates much heat [8–18]. The thermal stability of Li_xCoO_2 is affected by the type, particle size and concentration of the electrolyte salts, which strongly depend on the content of the electrolyte [12]. It is also well known that the fully lithiated graphite anode is unstable, which is attributed to the fact that the intercalated lithium can react with the electrolyte at the elevated temperature [16,19–22]. So far, almost all the studies on the thermal stability of Li_xCoO_2 and lithiated graphite anode are limited to the effects of the electrolyte. This is due to the fact that the electrolyte not only can react severely with the lithiated graphite anode at high temperature, but can also react easily with the O_2 evolved from the charged cathode. There are no studies on the effects of the atmosphere on the thermal stability of Li_xCoO_2 cathode and graphite anode. The atmosphere is an important factor which could significantly influence the thermal stability of Li_xCoO_2 and lithiated graphite. During the production

* Corresponding author. Tel.: +86 769 83015365.
E-mail address: hezuzhang_2000@163.com (Y.-B. He).

0040-6031/$ – see front matter © 2008 Elsevier B.V. All rights reserved.
doi:10.1016/j.tca.2008.09.019

process of batteries, although various measures have been taken to drive out the air in the batteries, it is inevitable that some air still exists in the batteries. Therefore, the analysis of the thermal stability of charged and discharged $LiCoO_2$ cathode and graphite anode in N_2 and air atmospheres is necessary for understanding the reaction mechanisms relating to safety. In this work, the thermal stability of charged and discharged $LiCoO_2$ cathode and graphite anode in N_2 and air atmospheres were investigated, and the effect of O_2 on the thermal stability of $LiCoO_2$ cathode and graphite anode was also examined.

2. Experimental

Lithium-ion batteries (model-463446, which was 4.6 mm thick, 34 mm wide and 46 mm long) were assembled. The batteries used $LiCoO_2$ as the cathode, graphite as the anode and polyethylene as a separator. The nominal capacity of the batteries was designed to be 800 mAh according to the theoretical specific capacity (274 mAh/g) and the actually available (reversible) specific capacity (137 mAh/g) of $LiCoO_2$. The $LiCoO_2$ cathodes consisted of 90 wt.% $LiCoO_2$, 5 wt.% conductive carbon black and 5 wt.% poly(vinylidene fluoride) (PVDF), and the graphite anodes consisted of 91 wt.% composite graphite, 6 wt.% styrene-butadiene rubber (SBR) and 3 wt.% carboxymethyl cellulose (CMC). 1 M $LiPF_6$ in a 1:1:1 (in mass) mixture of ethylene carbonate (EC), dimethyl carbonate (DMC) and ethylene methyl carbonate (EMC) (1 M $LiPF_6$/EC + DMC + EMC) was used as the electrolyte. The mass of pure $LiCoO_2$ of each battery was calculated, and the designed capacity of the graphite anodes and electrolyte was 2% larger than that of the $LiCoO_2$ cathodes, which could make the capacity of the $LiCoO_2$ cathodes being used completely. The preparation and injection of the electrolyte were conducted in an argon filled glove box.

The formation and charge/discharge tests were performed by the BS-9300 lithium-ion battery tester. Since the most recent industrial formation process constitutes only one cycle, the experimental batteries in this work also first underwent one cycle of charge/discharge for the formation. The batteries were charged with a constant current of 40 mA (0.05C) to 3.00 V, 80 mA (0.1C) to 3.85 V, and 160 mA (0.2C) to 4.20 V, followed by holding the voltage at 4.20 V until the current dropped to 8 mA (0.01C), and then discharged at 400 mA (0.5C) to 2.75 V of the cut-off voltage. After the formation, all batteries were charged and discharged two times between 2.75 and 4.20 V at a current of 400 mA (0.5C), which could stabilize the performance of batteries. The batteries with similar properties were chosen as the studied batteries. Some batteries were fully charged, and the others were fully discharged. The charged and discharged batteries were transferred to the glove box and then dissembled. The lithiated graphite was taken from the surface of anodes and the charged $LiCoO_2$ cathode from the surface of cathodes in the charged batteries. The de-lithiated graphite and discharged $LiCoO_2$ cathode were also taken from the fully discharged batteries. All the samples were rinsed with DMC to remove the electrolyte from the surface of the materials. Then, the samples were dried in the glove box antechamber for 2 h to remove the residual DMC. After the samples were dried, an appropriate amount of the samples (about 10 mg) were set in a stainless steel pan and were covered (not sealed) fitly by a circular stainless steel plate. The stainless steel pan with the samples was taken out from the glove box and introduced into the furnace of the TG-DTA immediately to conduct the TG-DTA experiments.

Some fully charged and discharged $LiCoO_2$ cathodes were heated from room temperature to different temperatures at 10 °C min^{-1} in air and N_2 atmospheres and the temperatures were kept for 1 h, and then the samples were cooled to room temperature.

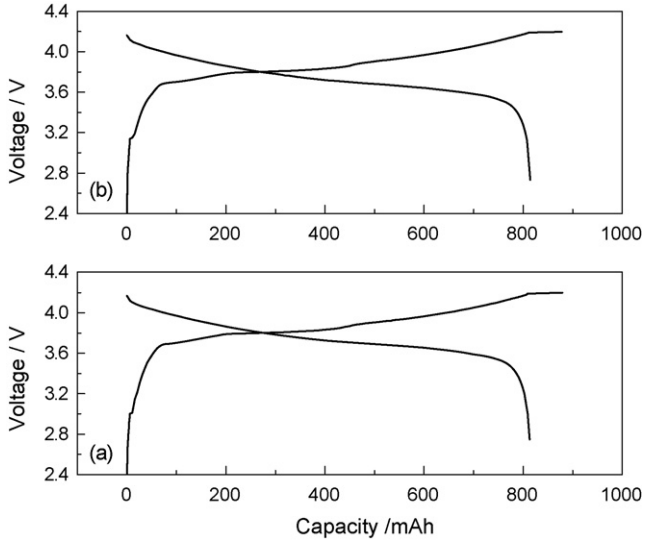

Fig. 1. The first charge and discharge curves for two batteries.

The X-ray diffraction (XRD) patterns of the pure $LiCoO_2$ and thermally treated fully discharged $LiCoO_2$ and fully charged $LiCoO_2$ were obtained by a PANAlytical X'Pert powder diffractometer using Co Ka radiation with an angular range of 10–90°(2θ) and a step of 0.02°(2θ) at room temperature. The structural parameters were calculated from the XRD patterns by using the MDI Jade 5.0 profile matching refinement method.

The thermogravimetric (TG) and differential thermal analysis (DTA) analyses for the $LiCoO_2$ cathode, graphite anode, conductive blank carbon and PVDF were conducted by using a Rigaku Thermo Plus TG8120 system. The stainless steel pan with samples was introduced into the furnace of the TG-DTA, and then the $LiCoO_2$ cathode, conductive black carbon and PVDF were heated to 800 °C at a rate of 10 °C min^{-1} and the graphite anode was heated to 450 °C at a rate of 5 °C min^{-1} under a nitrogen or air flow with Al_2O_3 as the reference material.

3. Results and discussion

The theoretical specific capacity of $LiCoO_2$ is 274 mAh/g and the available (reversible) specific capacity of $LiCoO_2$ is 137 mAh/g. However, the actual specific capacity of $LiCoO_2$ in commercial lithium-ion batteries depends on the material compositions of the anode, cathode, electrolyte and separator etc. Fig. 1 shows the first charge and discharge curves for two batteries. The capacities of the first charge and discharge of battery *a* are respective 879.10 and 813.19 mAh, and the capacities of battery *b* are respective 877.97 and 814.40 mAh. So the coulombic efficiency of these two batteries in the first cycle is 92.50% and 92.75%, respectively, which indicates that the electrochemical performance of these two batteries is quite similar. Thus, these two batteries can be used as the studied batteries. The mass of pure $LiCoO_2$ of batteries *a* and *b* is 5.819 and 5.823 g, respectively. So the actually available (reversible) specific capacity of $LiCoO_2$ in battery *a* is 139.75 mAh/g, and for battery *b* it is 139.85 mAh/g. After the formation, all the batteries were charged and discharged two times between 2.75 and 4.20 V at a current of 400 mA (0.5 C) to stabilize the performance of the batteries. The coulombic efficiency of these two batteries is over 99.70% in the two cycles. So it is reasonable to conclude that the coulombic efficiency is almost 100% if the batteries are cycled between 2.75 and 4.20 V. During the experiments, the battery *a* was fully charged and battery *b* was fully discharged, and then they were transferred into

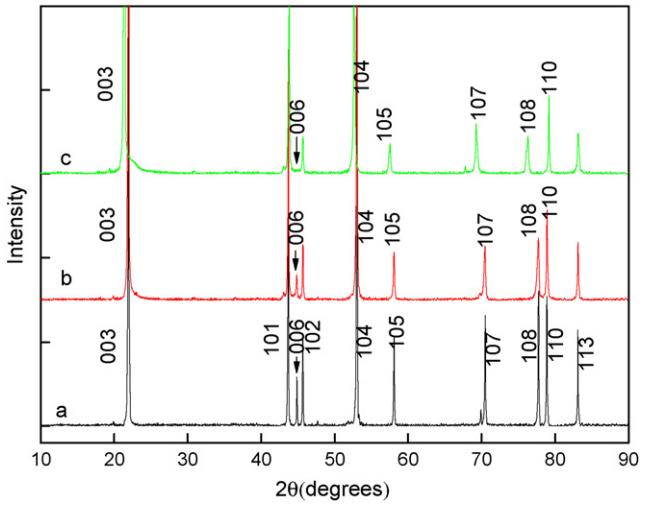

Fig. 2. XRD patterns of: (a) pure $LiCoO_2$, (b) fully discharged $LiCoO_2$ cathode, (c) fully charged $LiCoO_2$ cathode.

the glove box and dissembled. Therefore, it can be calculated that the actual value of x in Li_xCoO_2 at the fully discharged state (2.75 V) after the initial discharge is 0.965 and the x value at the fully charged state (4.20 V) is 0.453.

Fig. 2 shows the XRD patterns of the pure $LiCoO_2$, fully discharged $LiCoO_2$ and fully charged $LiCoO_2$ at room temperature. In all cases, the observed diffraction lines can be indexed based on the *R*-3*m* space group and are consistent with the layered structure of α-$NaFeO_2$. The hexagonal lattice parameters for the respective materials are a_h = 2.8163 Å, c_h = 14.0541 Å for the pure $LiCoO_2$; a_h = 2.8153 Å, c_h = 14.0653 Å for the fully discharged $LiCoO_2$; and a_h = 2.8084 Å, c_h = 14.4415 Å for the fully charged $LiCoO_2$. An expansion of the c_h parameter and a shrinkage of the a_h parameter for the delithiated material are observed as compared with those for the fully lithiated material.

As compared with the discharged $LiCoO_2$, there are three major different XRD characteristics for the charged $LiCoO_2$: (1) the (0 0 6) line almost disappears from the XRD of the delithiated (charged) $LiCoO_2$; (2) the (1 0 8) and (1 1 0) peaks for the delithiated (charged) $LiCoO_2$ are clearly separated by 2°(2θ); and (3) the (0 0 3), (1 0 4), (1 0 5) and (1 0 7) lines for the delithiated (charged) $LiCoO_2$ shift toward the lower 2θ angles. These results show that the microstructure of $LiCoO_2$ changes with the change from the charged state to the discharged state.

Fig. 3 shows the TG and DTA curves of conductive carbon black in N_2 and air atmospheres. An insignificant difference is observed when the tests are performed in N_2 and air atmospheres. It can be obviously observed from Fig. 3 that the carbon black sample is very stable in two atmospheres till the temperature is as high as 450 °C. Fig. 3(a) shows that there is little weight loss between 500 and 600 °C, while a weight loss of about 28 wt.% is observed in Fig. 3(b) from 450 to 600 °C. The weight loss is corresponding to the combustion of carbon black in air atmosphere, and an exothermic peak is also found on the DTA curve [23].

Fig. 4 presents the TG and DTA curves of PVDF in N_2 and air atmospheres for evaluating the thermal stability of the PVDF samples. It is observed from the TG curve that the PVDF sample is very stable till 400 °C. The weight of the sample decreases greatly after 400 °C, and the residue obtained is 12 and 22 wt.% in N_2 and air atmospheres, respectively. This is due to the decomposition of PVDF at high temperature. An endothermic behavior is found at the beginning of the degradation process, and then two exothermic peaks are observed on the DTA curves, which are at 500 and 600 °C for N_2 atmosphere and 470 and 550 °C for air atmosphere, respectively [16]. During the thermal degradation of PVDF, the C–H bond scission primarily occurs, which is due to the weaker bond strength of C–H (410 kJ/mol) when compared with that of C–F (460 kJ/mol) [24]. It is interesting to note that the decomposition of PVDF in N_2 atmosphere is more severe than that in air atmosphere.

Fig. 5 shows the TG and DTA curves of the fully charged cathode ($Li_{0.453}CoO_2$) in N_2 and air atmospheres. The decrease in the sample weight is around 3.0 wt.% between 100 and 120 °C in two atmospheres. The electrochemical oxidation of the solvent of the electrolyte solution, such as EC, DMC and EMC, occurs even at 3.80 V versus Li/Li^+ on the fresh $LiCoO_2$ during the first charge–discharge cycling. So a surface film is formed on the electrode surface, which is composed of multi-layers with inorganic and organic components [25]. The surface film on $LiCoO_2$ is not very stable and is thinner than that for the negative electrode. The surface state of $LiCoO_2$ has a significant influence on the stability of the decomposition products on the electrode surface [25–30]. Thus, the weight loss is attributed to the decomposition of the surface film components on the cathode, which might release some organic gases.

Another obvious weight loss of about 4.0 wt% is also observed from the TG curve at temperatures ranging from 240 to 300 °C, and the DTA curve shows a corresponding sharp exothermic peak at 250 °C. The fully charged cathodes consist of $Li_{0.453}CoO_2$, carbon black and PVDF. Figs. 3 and 4 have shown that the carbon black and PVDF samples are very stable till temperatures are as high as 450 and 400 °C in N_2 and air atmospheres, respectively. So the weight loss is not attributed to the combustion of the carbon black and the thermal degradation of PVDF.

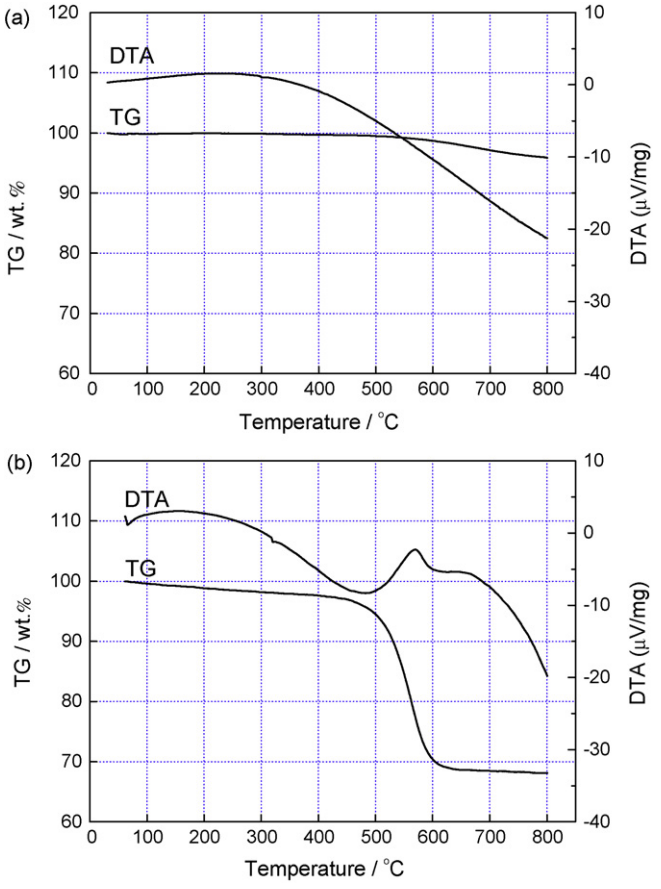

Fig. 3. TG and DTA curves of conductive carbon black: in N_2 atmosphere, (b) in air atmosphere.

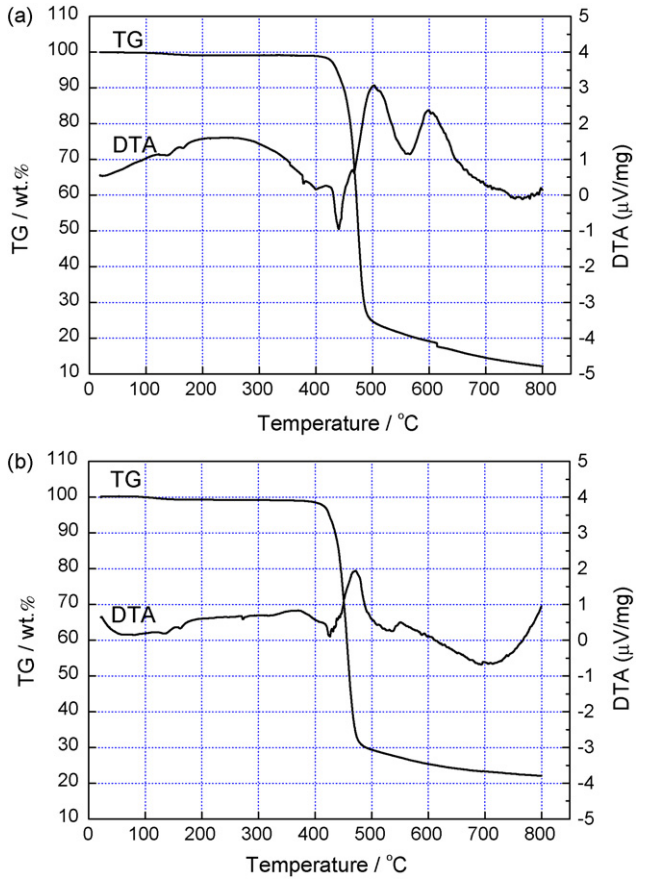

Fig. 4. TG and DTA curves of PVDF: (a) in N_2 atmosphere, (b) in air atmosphere.

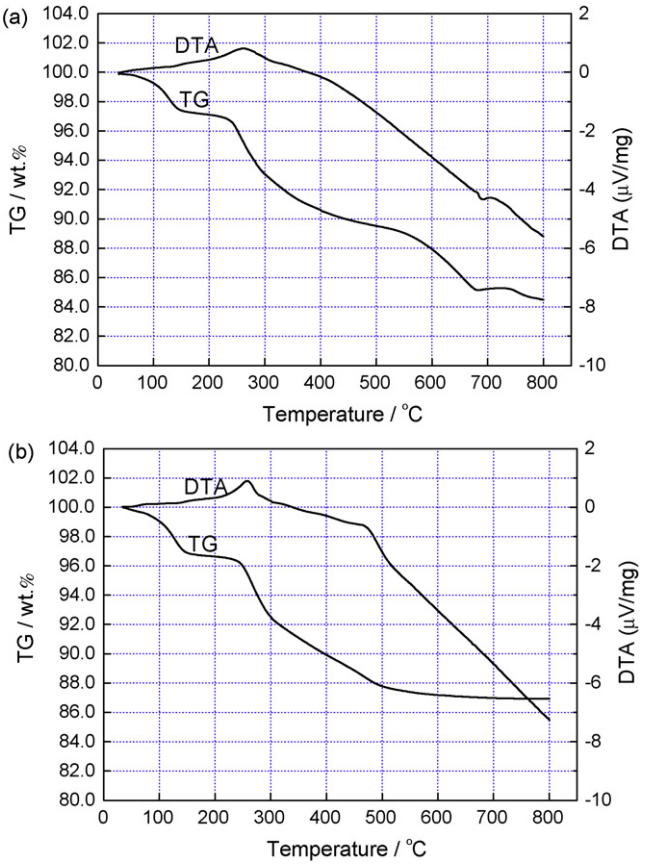

Fig. 5. TG and DTA curves of fully charged cathode ($Li_{0.453}CoO_2$): (a) in N_2 atmosphere, (b) in air atmosphere.

Fig. 6 shows the XRD patterns of the thermally treated fully charged cathode ($Li_{0.453}CoO_2$) at different temperatures and atmospheres. It can be seen that the XRD patterns of the fully charged cathodes treated at high temperature in air atmosphere is identified as a mixture of hexagonal $LiCoO_2$ (*R*-3*m*) and nonstoichiometric spinel Co_3O_4 (*Fd*3*m*). These experimental results suggest that the exothermic reaction starting at 250 °C is caused by the phase transition from the layered structure to the spinel structure. Thus, it can be concluded from the above results that the decomposition of $Li_{0.453}CoO_2$ may occur at 250 °C and the products are the $LiCoO_2$, Co_3O_4 and O_2 [17].

There is a further weight loss from 300 to 500 °C on the TG curve, the weight loss in N_2 atmosphere is less than that in air atmosphere, especially between 400 and 500 °C. The rate of weight loss decreases and an endothermic behavior is observed. The decomposition of $LiCoO_2$ does not occur below 850 °C in air atmosphere and Co_3O_4 can be transformed to CoO above 895 °C [31,32]. It also can be observed from Fig. 6 that the peak intensity corresponding to the Co_3O_4 phase increases as the thermal treatment temperature increases from 250 to 800 °C in air atmosphere, which indicates that the amount of Co_3O_4 phase increases with the rise of temperature. Fig. 6 also shows that the reaction products of fully charged cathode in air atmosphere do not contain the CoO samples. The fully charged cathode consists of $Li_{0.453}CoO_2$, carbon black and PVDF. The combustion of carbon black in air atmosphere occurs between 450 and 600 °C. So the Co_3O_4 as the decomposition products of fully charged cathode can not be reduced to CoO by carbon black below 500 °C in air and N_2 atmosphere.

Thus, the weight loss from 300 to 500 °C in air atmosphere results from the further decomposition of fully charged cathode, the thermal degradation of PVDF and the combustion of some carbon black. The weight loss from 300 to 500 °C in N_2 atmosphere is mainly attributed to the further decomposition of fully charged cathode and the thermal degradation of PVDF. So the combustion of carbon black in air atmosphere is the reason that the weight loss from 300 to 500 °C in air atmosphere is higher than that in N_2 atmosphere.

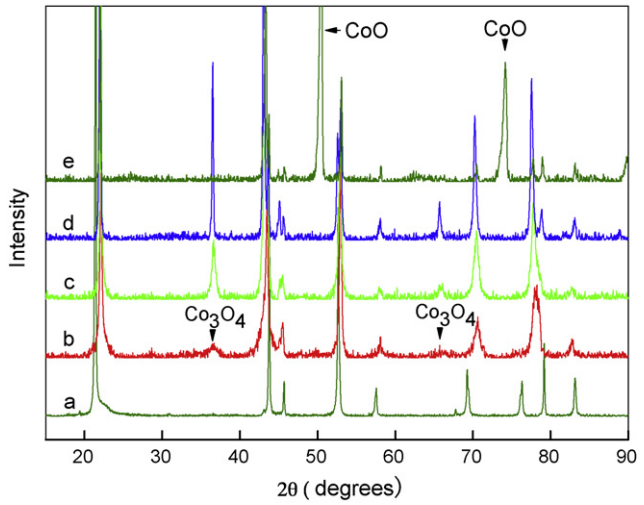

Fig. 6. XRD patterns of thermally treated fully charged cathode ($Li_{0.453}CoO_2$) at different temperatures and atmospheres: (a) room temperature in air atmosphere, (b) 250 °C in air atmosphere, (c) 400 °C in air atmosphere, (d) 800 °C in air atmosphere, (e) 800 °C in N_2 atmosphere.

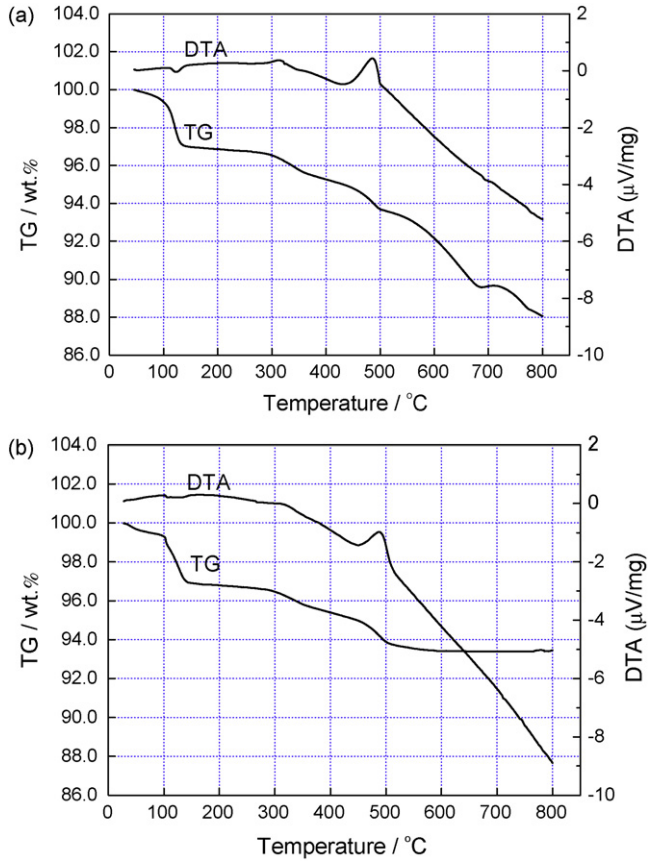

Fig. 7. TG and DTA curves of fully discharged cathode ($Li_{0.965}CoO_2$): (a) in N_2 atmosphere, (b) in air atmosphere.

Fig. 5 also presents that there is almost no weight change in the TG curves after 600 °C in air atmosphere, while the sample weight continues to decrease in N_2 atmosphere. Fig. 6(e) also shows that the reaction products of fully charged cathode in N_2 atmosphere at 800 °C are $LiCoO_2$ and CoO. It is well known that the decomposition of pure $LiCoO_2$ and Co_3O_4 does not occur below 850 °C in air atmosphere [31,32]. The PVDF has been decomposed and the black carbon has been combusted below 600 °C in air atmosphere. So the sample weight does not change in air atmosphere above 600 °C. While in N_2 atmosphere, the PVDF has been decomposed, but the black carbon has not been combusted below 600 °C. So the black carbon might be the factor which result in the sample weight loss above 600 °C in N_2 atmosphere. The Co_3O_4 as the decomposition product of cathode can be reduced to CoO by black carbon above 600 °C.

The decomposition and reduction reactions may be as follows:

$$Li_{0.453}CoO_2 \rightarrow 0.453LiCoO_2 + 0.182Co_3O_4 + 0.366O_2$$

$$Co_3O_4 + 1/2C \rightarrow 3CoO + 1/2CO_2$$

Fig. 7 presents the TG and DTA curves of the fully discharged $LiCoO_2$ cathode in N_2 and air atmospheres, respectively. The sample weight decreases to around 97 wt.% between 100 and 120 °C in two atmospheres. The DTA curve shows a small endothermic sharp peak, which indicates the decomposition of the surface film. When the sample temperature reaches 300 °C, the sample weight is further decreased to 96 wt.% from 300 to 400 °C, and an endothermic behavior is also observed.

Fig. 8 shows the XRD patterns of the thermally treated fully discharged cathodes ($Li_{0.965}CoO_2$) at different temperatures and

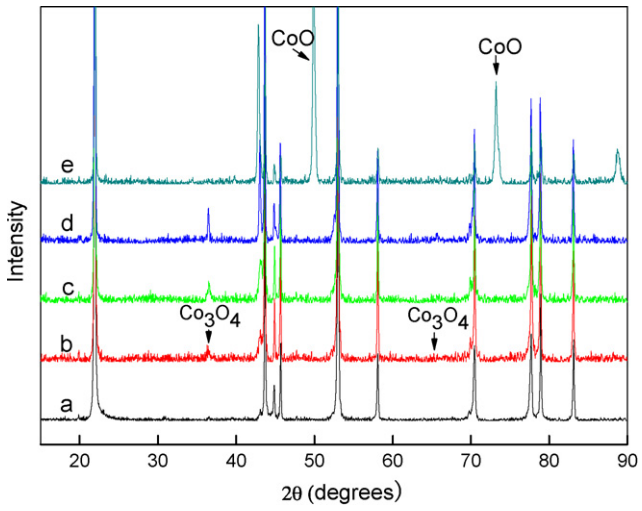

Fig. 8. XRD patterns of the thermally treated fully discharged cathode ($Li_{0.965}CoO_2$) at different temperatures and atmospheres: (a) room temperature in air atmosphere, (b) 250 °C in air atmosphere, (c) 400 °C in air atmosphere, (d) 800 °C in air atmosphere, (e) 800 °C in N_2 atmosphere.

atmospheres. It can be seen that the XRD patterns of the discharged cathodes treated at high temperature in air atmosphere are identified as a mixture of hexagonal $LiCoO_2$ (R-3m) and nonstoichiometric spinel Co_3O_4 ($Fd3m$). These experimental results suggest that the exothermic reaction starting at 300 °C is caused by the phase transition from the layered structure to the spinel structure. So the

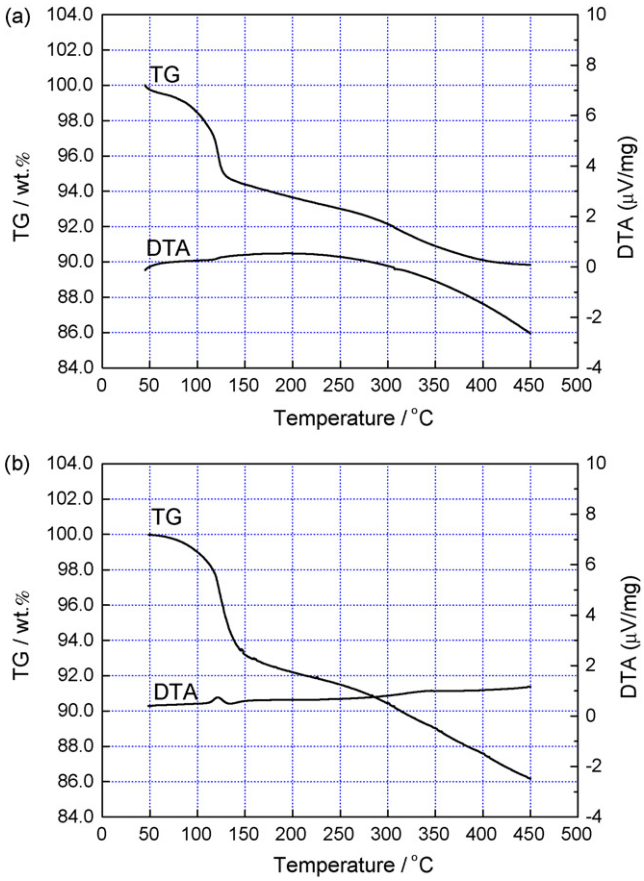

Fig. 9. TG and DTA curves of fully discharged graphite anode: (a) in N_2 atmosphere, (b) in air atmosphere.

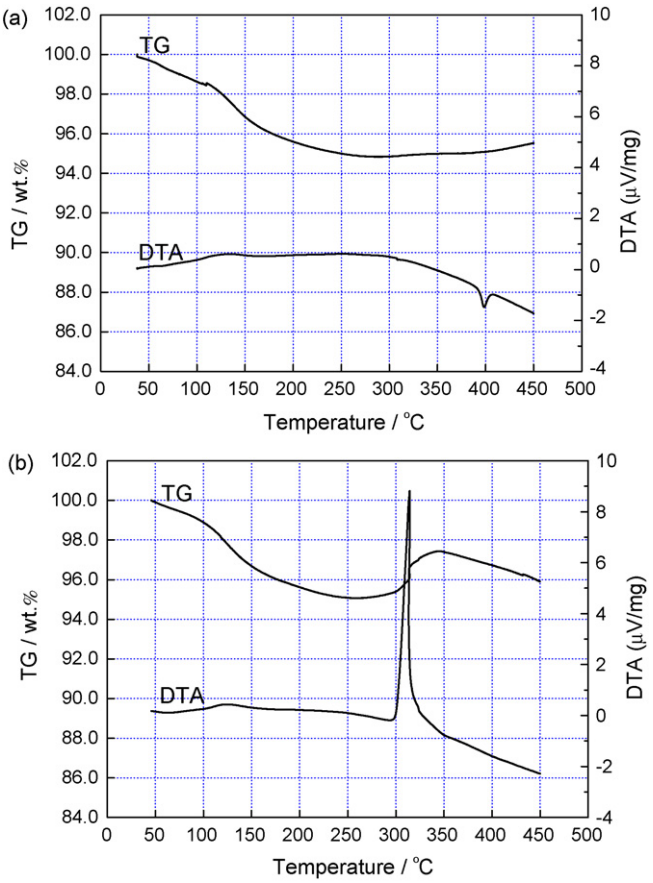

Fig. 10. TG and DTA curves of fully charged graphite anode: (a) in N_2 atmosphere, (b) in air atmosphere.

weight loss from 300 to 400 °C is attributed to the decomposition of $Li_{0.965}CoO_2$ with the products of $LiCoO_2$, Co_3O_4 and O_2 [17].

A weight loss and an exothermic peak are observed from 400 to 500 °C. Fig. 8 also shows that the amount of Co_3O_4 phase in air atmosphere increases with the increase of thermal treatment temperature. Thus, the weight loss from 400 to 500 °C in air atmosphere results from the further decomposition of fully discharged cathode, the thermal degradation of PVDF and the combustion of some carbon black. The weight loss from 400 to 500 °C in N_2 atmosphere is mainly attributed to the further decomposition of fully discharged cathode and the thermal degradation of PVDF.

Fig. 7 also presents that there is almost no weight change in the TG curves after 600 °C in air atmosphere, while the sample weight continues to decrease in N_2 atmosphere. Fig. 8(e) also shows that the reaction products of fully discharged cathode in N_2 atmosphere at 800 °C are $LiCoO_2$ and CoO. This is because the Co_3O_4 as the decomposition product of cathode can be reduced to CoO by black carbon in N_2 atmosphere above 600 °C.

Compared with the Figs. 6 and 8, we can learn that the amount of Co_3O_4 as the decomposition product of fully charged cathode ($Li_{0.453}CoO_2$) is obvious larger than that of fully discharged cathode ($Li_{0.965}CoO_2$). Figs. 5 and 7 also shows that the initial decomposition temperature of $Li_{0.453}CoO_2$ is higher than that of $Li_{0.965}CoO_2$. Thus, the thermal stability of the fully charged cathode is reduced greatly than that of the discharged cathode.

Fig. 9 shows the TG and DTA curves of the discharged graphite anode in N_2 and air atmospheres, respectively. The TG curve presents an obvious weight loss of about 7.0 wt.% from 100 to 120 °C, which is attributed to the decomposition of SEI film on the anode surface [3,22,33,34]. It is interesting to note that the weight loss of samples in air atmosphere is larger than that in N_2 atmosphere, which indicates that the thermal stability of SEI film in air atmosphere is worse than that in N_2 atmosphere. The sample weight decreases slowly with the increase in temperature in two atmospheres. An endothermic behavior is observed in N_2 atmosphere, while there is a sort of exothermic behavior in air atmosphere. In general, these two behaviors are not violent, so the thermal stability of the discharged graphite anode is excellent.

Fig. 10 shows the TG and DTA curves of the fully charged graphite anode in N_2 and air atmospheres, respectively. The TG curve shows that the sample weight decreases to around 97.0 wt.% from 100 to 120 °C and an exothermic behavior is also observed from the DTA curve, which is due to the decomposition of SEI film on the anode surface. The weight loss of the fully charged graphite anode is obviously less than that of the discharged graphite anode. When the batteries are fully charged, the lithium ions are intercalated into graphite layers. Some of the lithium ions are deposited and lithium metal is formed on the surface of graphite anodes. The lithium metal can be oxidized to Li_2O, which covers on the surface of graphite anodes and might restrain the decomposition of SEI film.

The sample weight does not change at around 300 °C in N_2 atmosphere, and the DTA curve shows an endothermic behavior. While in air atmosphere, the DTA curve shows an exothermic sharp peak at 300 °C, and the sample weight increases greatly. The main difference between the N_2 and air atmosphere is the O_2 in air atmosphere. Fig. 9(b) shows that the sample weight does not change obviously at 300 °C, and the DTA curve does not show any exothermic peak. This indicates that the graphite can not be oxidized to CO_2 at 300 °C in air atmosphere. So the exothermic reaction of the lithiated graphite anodes with O_2 occurs rapidly in air atmosphere, and the lithium metal in the graphite layer is oxidized to Li_2O.

4. Conclusions

The thermal stability of the fully charged and discharged $LiCoO_2$ cathode and graphite anode in nitrogen and air atmospheres was investigated by the thermogravimetric (TG) and differential thermal analysis (DTA). It was found that the thermal stability of the fully charged $LiCoO_2$ cathode was reduced greatly than that of the discharged $LiCoO_2$ cathode in two atmospheres. The exothermic decomposition reaction of the fully charged $LiCoO_2$ cathode occurred at 250 °C, while the decomposition reaction of the discharged $LiCoO_2$ cathode occurred at 300 °C. The sample weight of the fully charged and discharged $LiCoO_2$ cathode did not change after 600 °C in air atmosphere; while in nitrogen atmosphere the weight was reduced further. The Co_3O_4 as the decomposition product of the cathodes could be reduced to CoO by the carbon black above 600 °C in N_2 atmosphere. The weight loss of the fully charged graphite anode at 100–120 °C was obviously less than that of the discharged graphite anode. There was no fierce exothermic reaction of the lithiated graphite anode in N_2 atmosphere at 300 °C; while in air atmosphere the exothermic reaction of the lithiated graphite anode with O_2 occurred rapidly.

Acknowledgement

This work was supported by the R&D programs of the Ministry of Science and Technology of Dongguan.

References

[1] J.-M. Tarascon, M. Armand, Nature 414 (2001) 359.
[2] F. Alessandrini, M. Conte, S. Passerini, P.P. Prosini, J. Power Sources 97–98 (2001) 768.

[3] R. Spotnitz, J. Franklin, J. Power Sources 113 (2003) 81.
[4] S.-i. Tobishima, K. Takei, Y. Sakurai, J.-i. Yamaki, J. Power Sources 90 (2000) 188.
[5] P. Biensan, B. Simon, J.P. Pérès, A.d. Guibert, M. Broussely, J.M. Bodet, F. Perton, J. Power Sources (1999) 906.
[6] T. Ohsaki, T. Kishi, T. Kuboki, N. Takami, N. Shimur, Y. Sato, M. Sekino, A. Satoh, J. Power Sources 146 (2005) 97.
[7] S. Hossain, Y.-K. Kim, Y. Saleh, R. Loutfy, J. Power Sources 161 (2006) 640.
[8] H. Maleki, J.N. Howard, J. Power Sources 137 (2004) 117.
[9] J. Jiang, J.R. Dahn, Electrochem. Commun. 6 (2004) 39.
[10] D.D. MacNeil, J.R. Dahn, J. Electrochem. Soc. 150 (2003) A21.
[11] D.D. MacNeil, T.D. Hatchard, J.R. Dahna, J. Electrochem. Soc. 148 (2001) A663.
[12] J. Jiang, J.R. Dahn, Electrochim. Acta 49 (2004) 2661.
[13] D.D. MacNeil, J.R. Dahna, J. Electrochem. Soc. 148 (2001) A1205.
[14] D.D. MacNeil, J.R. Dahn, J. Electrochem. Soc. 149 (2002) A912.
[15] Y. Shigematsu, S.-i. Kinoshita, M. Ue, J. Electrochem. Soc. 153 (2006) A2166.
[16] J.-i. Yamaki, Y. Baba, N. Katayama, H. Takatsuji, M. Egashira, S. Okada, J. Power Sources 119–121 (2003) 789.
[17] Y. Baba, S. Okada, J.-i. Yamaki, Solid State Ionics 148 (2002) 311.
[18] J.R. Dahn, E.W. Fuller, M. Obrovac, U.v. Sacken, Solid State Ionics 69 (1994) 265.
[19] D.D. MacNeil, D. Larcher, J.R. Dahn, J. Electrochem. Soc. 146 (1999) 3596.
[20] J. Jiang, J.R. Dahn, Electrochim. Acta 49 (2004) 4599.
[21] A. Xiao, W. Li, B.L. Lucht, J. Power Sources 162 (2006) 1282.
[22] J.-i. Yamaki, H. Takatsuji, T. Kawamura, M. Egashira, Solid State Ionics 148 (2002) 241.
[23] M. Bokova, C. Decarne, E. Abi-Aad, A. Pryakhin, V. Lunin, A. Aboukäıs, Appl. Catal. B: Environ. 54 (2004) 9.
[24] G. Botelho, S. Lanceros-Mendez, A.M. Gonçalves, V. Sencadas, J.G. Rocha, J. Non-Cryst. Solids 354 (2008) 72.
[25] T. Matsushita, K. Dokko, K. Kanamura, J. Power Sources 146 (2005) 360.
[26] X. Wang, T. Hironaka, E. Hayashi, C. Yamada, H. Naito, G. Segami, Y. Sakiyama, Y. Takahashi, K. Kibe, J. Power Sources 168 (2007) 484.
[27] M. Hirayama, N. Sonoyama, T. Abe, M. Minoura, M. Ito, D. Mori, A. Yamada, R. Kanno, T. Terashima, M. Takano, K. Tamura, J.i. Mizuki, J. Power Sources 168 (2007) 493.
[28] M. Matsui, K. Dokko, K. Kanamura, J. Power Sources. (2007).
[29] D. Aurbach, B. Markovsky, G. Salitra, E. Markevich, Y. Talyossef, M. Koltypin, L. Nazar, B. Ellis, D. Kovacheva, J. Power Sources 165 (2007) 491.
[30] R. Dedryvère, H. Martinez, S. Leroy, D. Lemordant, F. Bonhomme, P. Biensan, D. Gonbeau, J. Power Sources 174 (2007) 462.
[31] E. Antolini, M. Ferretti, J. Solid State Chem. 117 (1995) 1.
[32] E. Antolini, Int. J. Inorg. Mater. 3 (2001) 721.
[33] L. Zhao, I. Watanabe, T. Doi, S. Okada, J.-i. Yamaki, J. Power Sources 161 (2006) 1275.
[34] I. Watanabe, J.-i. Yamaki, J. Power Sources 153 (2006) 402.